

JOURNAL OF THE AMERICAN CHEMICAL SOCIETY

Registered in U. S. Patent Office. © Copyright 1974 by the American Chemical Society

VOLUME 96, NUMBER 8

APRIL 17, 1974

Medium Effects on Heavy-Atom Kinetic Isotope Effects. III. Structured Medium Model Applied to Complex Formation *via* Mass Point Attachment and Coupling

Joseph H. Keller and Peter E. Yankwich*

*Contribution from the Noyes Laboratory of Chemistry, University of Illinois,
Urbana, Illinois 61801. Received September 11, 1973*

Abstract: A structured medium model (SMM) for reactant-medium interactions is defined and applied to calculation of heavy-atom kinetic isotope effects in the reaction of a three-particle molecule as influenced by attachment (and coupling) of one and two mass points. The results for this simplest model of complex formation with uni- and bidentate ligands are compared with those obtained previously with a cell model (CMM) treatment of reactant-medium interactions, several different flat-barrier reaction coordinates being tested. A number of different methods were tried for handling the problem of redundant internal coordinate sets; such redundancies are commonplace in intramolecular hydrogen bonding and whenever cycles are produced by bonds among particles. SMM effects on the temperature-dependent factor in an isotopic rate constant ratio are larger at comparable force constant levels than those obtained *via* CMM. Interactions sufficiently weak that a reactant-ligand complex forms without alteration of the reaction coordinate or diagonal force field of the reagent yield isotope effects within the framework of SMM which could be measured in careful comparison experiments, while those predicted by CMM would be undetectable. The SMM generates substantial effects on the temperature-independent factor in the isotopic rate constant ratio which have no counterpart in CMM. Comparison of related intermolecular and intramolecular kinetic isotope effects should be especially useful in estimating actual complexing and/or medium effects and in discovering the conditions under which CMM or SMM is the better model.

This paper is the third in a series of reports of computational studies of medium effects on heavy-atom kinetic isotope effects. Earlier, the cell model, or "continuous medium method" (hereinafter CMM), developed and used for the study of vapor pressure isotope effects by Stern, Van Hook, and Wolfsberg,¹ was applied to model calculations for decompositions (*via* several reaction coordinates) of a hypothetical nonlinear triatomic molecule (hereinafter TAM), formic acid, and oxalic acid, under conditions of no interactions among internal coordinates of the reactant and the external translational rotational coordinates characteristic of this approach; later, similar studies were made of TAM with external-external and certain external-internal coordinate interactions (specifically, ones in which the internal coordinate was not a component of the reaction coordinate).² Values of the diagonal external force constants were adjusted to yield associated frequencies typical of moderate hydrogen bonding (30–90 cm⁻¹).

(1) M. J. Stern, W. A. Van Hook, and M. Wolfsberg, *J. Chem. Phys.*, **39**, 3179 (1963).

(2) J. H. Keller and P. E. Yankwich, *J. Amer. Chem. Soc.*, **95**, 4811, 7968 (1973).

In no case studied were the medium effects on calculated ¹³C kinetic isotope effects of sufficient size to be experimentally measurable given present techniques; for molecules of ordinary mass and complexity, the effects predicted would likely not even be detectable. The additivity of the effects, subject to certain restrictions, made it possible to list the conditions for production of medium effects of experimentally significant magnitudes within the framework of the CMM: (i) the isotopic molecules should be relatively small and light; (ii) reaction temperatures should be low (say, below 25°); (iii) solvent-solute interactions should be drastically different in the reactant and transition states; (iv) one or more of the component interactions should include coupling to an internal coordinate (preferably isotopic) which is part of the reaction coordinate; and (v) the force constants associated with such interactions should yield related vibrational frequencies of several hundred reciprocal centimeters.

The latter pair of conditions strains the assumptions of the CMM, which provide for a generalized effect by the medium on the reactant but which do not include

structural features for the medium. Since elements of structure seem usually to be associated with strong interactions, our attention was turned to an opposite of CMM in which the reactant is embedded in a medium composed of an organized system of particles. In full form, this structured medium model (hereinafter SSM) would employ a group of particles sufficiently large that edge effects would be nil and the behavior induced by the finite set accurately reflective of that arising in an infinite set. To reduce the computation to a more tractable magnitude, an approximation is employed in which the reactant(s) and a portion of the surrounding medium are treated formally as if they were a single molecule. (Kresge, *et al.*,³ have used a similar technique to calculate solvent isotope effects for reactions of H_3O^+ in H_2O .) By this device one can imitate the restricted motions of reactant molecules in a medium of variable rigidity and density, and localized interactions and molecular properties of the medium can both be handled. In this form of SMM the approximation arises principally in the fact that certain mass-determined elements of the structure-related input may have unrealistic values because the internal coordinate definitions are those of a single grand molecule rather than of a molecular assembly.

This paper reports the first stage of a study of the SMM. Here, one and two mass points are attached to the end atoms of TAM and then to each other. Coupling of attached mass points can create a problem for kinetic isotope effect calculations, absent from those for equilibrium isotope effects, by making redundant the set of internal coordinates employed for the kinematic description of the transition state. The magnitude of this problem is assessed and methods are developed for its reduction.

Essentially, this is an investigation of the effects of incorporation of the reactant into complexes with structureless uni- and bidentate ligands. TAM was chosen rather than a realistic molecular model because the expected effects should be maximum with it, and earlier work permits an estimate of effects for a larger, more complex reactant to be made from those observed with TAM. A main purpose of this investigation was determination of the size of medium-induced isotope effects one might expect in the SMM, since such apparently are trivial in the CMM for isotopes of atoms as heavy as carbon. A secondary purpose was to learn the influence on SMM medium-induced isotope effects of parameter variations of reasonable magnitude and span. Such results suggest the ways in which one might test for and estimate through experiment medium-induced components of kinetic isotope fractionation.

I. Methods and Models

A. Computations. All calculations were carried out within the framework of transition state theory. Reactant and transition state eigenvalues and eigenvectors for light- and heavy-isotopic species were calculated using Schachtschneider and Snyder's programs⁴ for solution of the Wilson GF matrix problem.⁵ The

(3) R. A. More O'Ferrall, G. W. Koepl, and A. J. Kresge, *J. Amer. Chem. Soc.*, **93**, 9 (1971).

(4) J. H. Schachtschneider and R. G. Snyder, *Spectrochim. Acta*, **19**, 177 (1965).

(5) E. B. Wilson, Jr., J. C. Decius, and P. C. Cross, "Molecular Vibrations," McGraw-Hill, New York, N. Y., 1955.

Table I. Input Parameters and Model Descriptions

A. Structural Elements and Reactant Basis Force Field —Internal coordinate—					
Designation, <i>i</i>	Description	Value	F_{ii}^0		
1	r_{ab}	1.54 Å	4.40 ^a		
2	r_{bc}	1.54 Å	4.40		
3	$\angle abc$	109.5°	1.63		
4	r_{am}	3.00 Å	v^b		
5	$\angle bam$	180°	v		
6	r_{en}	3.00 Å	v		
7	$\angle bcn$	180°	v		
8	r_{mn}	7.41 Å	v		
B. Isotope Effects (Mass Patterns of Reactant) ^c					
Description		m_c	m_b	m_a	Designation of k/k'
Intermolecular, a isotopic	k	12	12	12	α
	k'	12	12	13	
Intermolecular, b isotopic	k	12	12	12	β
	k'	12	13	12	
Intramolecular	k	13	12	12	γ
	k'	12	12	13	
C. Models					
"Atoms" a, b, c, plus	Coordinates defined, 1, 2, 3, plus	Representation		"Structure" designation	
None	None			A	
m	4, 5			B	
n	6, 7			C	
n, m	4, 5, 6, 7			D	
n, m	4, 6			E	
n, m	4, 5, 6, 7, 8			F	
n, m	4, 6, 8			G	
n, m	4, 5, 7, 8			H	
D. Attached Masses ^c					
Mass associated with m and/or n		Designation			
4		J			
16		K			
56		L			
150		M			
E. Varied Force Constants					
Identification	Value	Designation			
F_{44}^0 and/or F_{66}^0 ^a	10 ⁻⁴	N			
	0.5	P			
	1.0	Q			
	1.5	R			
F_{53}^0 and/or F_{77}^0	5 × 10 ⁻⁵	N			
	0.25	P			
	0.50	Q			
	0.50	R			
F_{88}^0	10 ⁻⁴	S			
	1	T			
	2	U			

^a Stretching force constants in mdyn/Å; bending force constants in mdyn/Å. ^b v = varied value. ^c Integer atomic masses.

Table II. Elements of the Matrices ΔG^a

j	i								j
	1	2	3	4	5	6	7	8	
	0.6410	-0.2132	-0.3916	0	0	0	0.3924	0	1
		0.6410	-0.3916	0	0.3924	0	0	0	2
1	0.6410		0.7172	0	0.3605	0	0.3605	0	3
2	0	0		0	0	0	0	0	4
3	0	0	0.2703		0.2703	0	0.0902	0	5
4	-0.6410	0	0	0.6410		0	0	0	6
5	0	0	-0.4901	0	0.6190		0.2703	0	7
6	0	0	0	0	0	0		0	8
7	0	0	0	0	0	0	0		
8	0	0	0	0	0	0	0	0	

^a Upper right, values of $10^3(G_{ij} - G_{ij}')$ for atom b isotopic; lower left, for atom a isotopic.

complete partition functions were computed using programs similar to those of Wolfsberg and Stern;⁶ in turn, these partition functions were used for calculation of the ratio of the isotopic specific rate constants k and k' .

$$k/k' = (\text{TIF})(\text{TDF}) \quad (1)$$

TIF is the ratio $\nu_1^\ddagger/\nu_1'^\ddagger$ associated with the reaction coordinate at the transition state; it is the high-temperature limit of k/k' , is independent of the genuine vibrations of the activated complex, and, for a given structure and mass pattern (*i.e.*, G and G'), depends only on the isotopic reaction coordinate eigenvectors. TDF is the ratio between the reactant and transition states of the isotopic partition function ratios involving the genuine vibrations of both. The two factors of k/k' are separated conveniently in logarithmic form, with $L(X) = 100 \ln(X)$

$$L(k/k') = L(\text{TIF}) + L(\text{TDF}) \quad (2)$$

and our discussion of temperature dependence will be through graphs of $L(\text{TDF})$ vs. $\theta = 1000/T^\circ\text{K}$.

B. Models. The basis TAM is taken as a symmetric nonlinear triad of "atoms" with masses of 12 integer atomic mass units; the isotopic molecules have one atom of mass 13. The internal coordinate designations, values of structural parameters, basic molecular force field, and isotope effect descriptions are listed in parts A and B of Table I; the planar structure of the models and the several internal coordinates are shown in Figure 1.

Modest variations in geometry are known⁷ to have small effects on kinetic isotope effects and were not investigated; the same structures were assumed for reactant (⁰) and transition ([‡]) states: $G^\ddagger \equiv G^0$. The decompositions are considered to be unimolecular; the consequences of bimolecular reaction pathways are the subject of another investigation presently underway.

Only in-plane internal coordinates are defined and only such are components of reaction coordinates. Under such conditions, out-of-plane coordinates contribute to potential energies but not to isotope effects and so are left undefined. The several combinations of "attached masses" and internal coordinates used in construction of G matrices are shown in part C of Table I, while the masses of the complexing particles m and n are listed in part D. With respect to the number of internal coordinates sufficient for description of a struc-

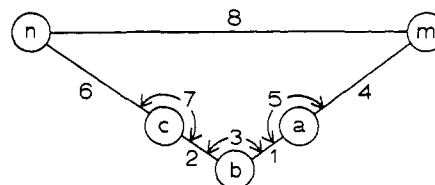


Figure 1. Internal coordinate designations; see Table IA.

ture in the molecular plane, coordinate set F is overdefined by one (redundant), E is underdefined by two and G by one, and the others are complete. As an aid in the interpretation of results, the elements of $\Delta G = (G - G')$ are collected in Table II.

The force constants listed in part E of Table I are those for the bond stretch and angle bend coordinates descriptive of the attachment of m to a and n to c and of the coupling of m to n . Unlike F_{11} , F_{22} , and F_{33} , the force constant values listed in part E are in poor correspondence with the appropriate interatomic distances, but this is merely another element of arbitrariness in the valuation of parameters and of no other significance. The values of these force constants are intended to be imitative of weak van der Waals interactions at the low extreme and of very strong (near valence bond level) interactions at the high.

A set of up to four letters from the lists of designations in parts C, D, and E of Table I will be used to identify the G and the various components of F in each model calculation. The first position is the structure designation A-H, the second is the level of attached atom masses J-M, the third is the level of "attachment" force constants N-R, and the fourth is the size of the coupling force constant F_{88} , S-U. The letters X, Y, and Z will be used in the second, third, and fourth positions, respectively, as dummies for a range of values of the parameters. Later, we shall employ a technique for "reduction" of the redundancy of structure F. Such a transformation will be indicated by using in the first position a group of symbols such as D/F; this means that the force field defined for G -matrix F was transformed to that appropriate for G -matrix D [and G -matrix D was actually employed in the calculation]. Such a transformation has no effect on reactant vibration frequencies or related isotope shifts.

C. Reaction Coordinates. Four reaction coordinates were studied: simple bond ruptures between atoms a and b (1) and b and c (2), and concerted displacements in these same internal coordinates which are symmetric (12+) and asymmetric (12-). Al-

(6) M. Wolfsberg and M. J. Stern, *Pure Appl. Chem.*, **8**, 225, 325 (1964).

(7) M. J. Stern and M. Wolfsberg, *J. Pharm. Sci.*, **54**, 849 (1965).

though none of the attachment or coupling coordinates are made components of a reaction coordinate, the results of computations with these four reaction coordinates can be used to estimate the consequences of such inclusion.

Where F^\ddagger is used as defined and untransformed, the transition states for simple bond rupture are generated by making the appropriate diagonal force constant zero, $F_{ii}^\ddagger = 0$; except for this difference, F^0 and F^\ddagger are the same. The two-element reaction coordinates 12+ and 12- become transition state normal modes when $F_{12}^\ddagger = \pm(F_{11}F_{22})^{1/2}$, the positive value yielding the asymmetric motion, etc.⁸

When F^0 is transformed to reduce the redundancy characteristic of structure F, it is no longer diagonal; in general $F_{ij}^0 \neq 0$ for all i and j . To generate a transition state, the transformed F^0 must be modified so that certain rows/columns of the resulting F^\ddagger are similar to those of an untransformed F^\ddagger . When the reaction coordinate is i , all force constants in row/column i are set to zero. When the reaction coordinate is $ij\pm$, F_{ij}^\ddagger is set to the properly signed geometric mean of the transformed F_{ii}^\ddagger and F_{jj}^\ddagger , which are left as is, and all other force constants in rows/columns i and j are set to zero.

These methods result in reaction coordinate eigenvalues which are zero, and the associated eigenvectors have only one or two, as the case may be, nonzero elements. (That is, these are calculations of types I and II.^{9,10})

D. The Problem of Redundant Coordinates. Calculations of kinetic isotope effects are often made with molecular models in which a complete nonredundant set of internal coordinates is defined. Sometimes, a cyclic transition state seems appropriate and a pair of originally terminal atoms are joined by a new "bond" (internal stretching coordinate), thus making the set of internal coordinates redundant.¹¹

Coordinate redundancy creates no particular problems when one is concerned with the wholly genuine manifold of vibrational normal modes. Provided the potential energy is invariant, a constant set of eigenvalues and eigenvectors will be obtained. Transition states present a problem only because of the nongenuine vibration which is the reaction coordinate. Application of the techniques described in section C above to situations in which there is redundancy in the set of internal coordinates results in a nonzero (but usually small) reaction coordinate eigenvalue and in an associated eigenvector having several nonzero elements in addition to those comprising the preselected reaction coordinate. Vogel and Stern¹¹ met the difficulty of $\nu_1^\ddagger \neq 0$ in type II calculations for over-defined cyclic transition states by adjusting the value of F_{ij}^\ddagger so that ν_1^\ddagger became zero; in many cases this procedure fails to eliminate the "contaminating" elements in the corresponding eigenvector. A more involved technique is required to eliminate effects of internal coordinate redundancy simultaneously on the reaction coordinate

eigenvalue and eigenvector. We have experimented with two such techniques: (i) coordinate elimination, sometimes to the point of under-definition of the system; and (ii) "reduction" of redundancy by transformation of F^\ddagger to correspond to a nonredundant G , a procedure based on those of Gold, Dowling, and Meister¹² and Hubbard.¹³ These techniques are necessary and the matter of coordinate redundancy of concern only if one attempts simultaneously to associate a particular "frequency" with the reaction coordinate motion and preselect the reaction coordinate eigenvector. One has had to treat the reaction coordinate eigenvector as a matter of moment since Bigeleisen and Wolfsberg¹⁴ and Johnston, Bonner, and Wilson⁸ focussed attention on its significance to the values of calculated kinetic isotope effects.

A set of internal coordinates of which one or more are redundant causes the same number of eigenvalues of G to be zero, and that number of related eigenvectors L_i from the set represented by the matrix L will be null vectors. Further, G^{-1} does not exist. If one does not require G^{-1} , this is no impediment, but most methods for development of F^\ddagger to yield a preselected reaction coordinate (whose eigenvalue and eigenvector we shall designate λ_1^\ddagger and L_1 , respectively) employ the relation

$$F^\ddagger L_1 = \lambda_1^\ddagger G^{-1} L_1 \quad (3)$$

In the special case (general here) of $\lambda_1^\ddagger = 0$, eq 3 becomes simply

$$F^\ddagger L_1 = 0 \quad (4)$$

but the existence of G^{-1} is implied, nevertheless, and the simple type I technique ($F_{ii}^\ddagger = 0$) and the simple type II ($F_{ij}^\ddagger = \pm(F_{ii}^\ddagger \cdot F_{jj}^\ddagger)^{1/2}$) yield neither $\lambda_1^\ddagger = 0$ nor simple L_1 .

Redundancy in this study arises when internal coordinate 8 is defined in addition to those of structure D so that F_{88} between m and n can be made nonzero;¹⁵ see Table IC. Table III exhibits for the resulting structure F the effects on λ_1^\ddagger and L_i for two simple reaction coordinates at each of two levels (N, P) of the complexing force constants. These levels of eigenvector contamination ($L_3, \dots, L_8 \neq 0$) are much greater than those which result from over-simplified attempts to introduce curvature into the potential barrier at the transition state;¹⁶⁻¹⁹ there is substantial motion in each case beyond the input simple bond rupture. The normal mode frequencies for the reactant (redundant or not, ν_{R,NR^0}) and for the F^\ddagger and G corresponding to structure F (ν_R^\ddagger) are shown in the first four columns of Table IV.

The work of Stern and Wolfsberg^{20,21} suggests that the introduction of F_{88} (structure D \rightarrow F) may have a small effect on isotope effects calculated for isotopy at atom a or b provided the reaction coordinate does not involve internal coordinates 4-8. Comparison of

(12) R. Gold, J. M. Dowling, and A. G. Meister, *J. Mol. Spectrosc.*, **2**, 9 (1958).

(13) R. L. Hubbard, *J. Mol. Spectrosc.*, **6**, 272 (1961).

(14) J. Bigeleisen and M. Wolfsberg, *J. Chem. Phys.*, **21**, 1972 (1953); **22**, 1264 (1954).

(15) J. C. Decius, *J. Chem. Phys.*, **17**, 1315 (1949).

(16) R. W. Kidd and P. E. Yankwich, *J. Chem. Phys.*, **59**, 2723 (1973).

(17) R. W. Kidd and P. E. Yankwich, *J. Chem. Phys.*, in press.

(18) G.-J. Wei and P. E. Yankwich, *J. Chem. Phys.*, in press.

(19) J. H. Keller and P. E. Yankwich, *J. Phys. Chem.*, **78**, 544 (1974).

(20) M. J. Stern and M. Wolfsberg, *J. Chem. Phys.*, **45**, 2618 (1966).

(21) M. J. Stern and M. Wolfsberg, *J. Chem. Phys.*, **45**, 4105 (1966).

(8) H. S. Johnston, W. A. Bonner, and D. J. Wilson, *J. Chem. Phys.*, **26**, 1002 (1957).

(9) T. T.-S. Huang, W. J. Kass, W. E. Buddenbaum, and P. E. Yankwich, *J. Phys. Chem.*, **72**, 4431 (1968).

(10) W. J. Kass and P. E. Yankwich, *J. Phys. Chem.*, **73**, 3722 (1969).

(11) P. C. Vogel and M. J. Stern, *J. Chem. Phys.*, **54**, 779 (1971).

Table III. Reaction Coordinate "Frequencies" and Eigenvectors Under Conditions of Redundancy ($\sum_i |L_i| = 1$)

	Model			
	FKNU		FKPU	
	Reaction coordinate			
	1	2	1	2
$\nu_1^\ddagger, \text{cm}^{-1}$	0.75	0.75	49.73	49.73
L_1	+0.668072 ^a	0.0	+0.676870 ^a	-0.001856
L_2	0.0	+0.668072 ^a	-0.001856	+0.676870 ^a
L_3	-0.000005	-0.000005	-0.026286	-0.026286
L_4	-0.009549	-0.020260	-0.008401	-0.017919
L_5	-0.141721	-0.159655	-0.123462	-0.139324
L_6	-0.020260	-0.009549	-0.017919	-0.008401
L_7	-0.159655	-0.141721	-0.139324	-0.123462
L_8	+0.000003	+0.000003	+0.005882	+0.005882

^a In the absence of redundancy, $L_i = 1.000000$ for these simple reaction coordinates and $\nu_1^\ddagger = 0$.

Table IV. Normal Mode Frequencies of Reactant (⁰) and Transition ([‡]) States^a

i, j	$(\nu_{R, NR^0})_i$	$(\nu_{R, NR^0})'_i$	$(\nu_{R^\ddagger})_j$	$(\nu_{R^\ddagger})'_j$	$(\nu_{NR^\ddagger})_j$	$(\nu_{NR^\ddagger})'_j$
1	1221.129	1211.471	1163.149	1162.843	1166.427	1166.048
2	1111.844	1100.447	690.645	689.206	951.490	942.531
3	688.520	687.616	658.724	654.094	643.036	636.362
4	594.845	585.665	332.706	326.181	315.617	312.777
5	308.277	306.648	248.262	246.485	201.215	198.199
6	194.694	191.668	192.376	188.246	183.487	181.589
7	181.111	179.743	(49.734) ^b	(49.459)	0.0 ^b	0.0
8	0.0 ^c	0.0	0.0 ^c	0.0		

^a ν_R , for FKPU, ν_{NR} for D/FKPU. Reaction coordinate is 1, atom a is isotopic. ^b Reaction coordinate frequency. ^c Redundancy null frequency, $L \equiv 0$.

Table V. Comparison of Elimination and Transformation Methods for Reducing Redundancy (Intermolecular Isotope Effect α , Reaction Coordinate 1)

	Model						
	DKP	EKP	FKPU ^{a-c}	GKPU	HKPU	D/FKPU	H/FKPU
$L(\text{TIF})$	0.8889	1.0569	0.5558	0.8545	0.4469	0.8889	0.4469
$L(\text{TDF}), \theta = 1$	0.3950	0.3950	0.3953	0.3950	0.3950	0.2741	0.3487
2	1.4074	1.4072	1.4083	1.4072	1.4074	0.9672	1.2290
3	2.7267	2.7255	2.7287	2.7254	2.7266	1.8586	2.3470
4	4.1491	4.1459	4.1521	4.1452	4.1481	2.8176	3.5180
5	5.5893	5.5842	5.5927	5.5817	5.5860	3.7967	4.6740

^a $\nu_1^\ddagger = 49.73 \text{ cm}^{-1}$; for all other cases, $\nu_1^\ddagger = 0$. ^b If L_1^\ddagger and ν_1^\ddagger are not treated as related to a reaction coordinate, $(k/k') = K_\alpha$, an isotope exchange equilibrium constant, for which $L(\text{TIF}) = 0$ and $L(K_\alpha) \equiv L(\text{TDF}) = 0.3950, 1.4074, 2.7266, 4.1484,$ and 5.5869 at the values of θ indicated. ^c FKNU; $\nu_1^\ddagger = 0.75 \text{ cm}^{-1}$, $L(\text{TIF}) = 0.5756$; $L(\text{TDF}) = 0.3968, 1.4305, 2.8149, 4.3556,$ and 5.9646 .

columns 1 (DKP) and 3 (FKPU) of Table V shows that, in spite of the proximity of coordinate 8 to atom a (the position of isotopy) and although there are major differences between the *actual* reaction coordinate motions in the two cases (see column 4 of Table III), the $L(\text{TDF})$'s differ only slightly; further, the $L(\text{TIF})$'s, though somewhat different, are not so large as to determine $L(k/k')$ except at temperatures well above 25° . (To a first approximation,²² $L(\text{TDF})$ here is proportional to $(F_{11}^0)\Delta G_{11}$, which is unaffected by the difference between structures D and F, while

$$L(\text{TIF}) = 100 \ln \left[\frac{\mathbf{L}_1^T(\mathbf{G}^{-1})'\mathbf{L}_1}{\mathbf{L}_1^T(\mathbf{G}^{-1})\mathbf{L}_1} \right]^{1/2} \quad (5)$$

many elements of which are so affected.) At least in this case, one could just ignore the redundancy problem provided the details of the reaction coordinate motion (\mathbf{L}_1) were of no interest. However, this approach is unsupportable if the objectives of reaction modeling go beyond data matching to include the development of chemical and physical insights.

(22) J. Bigeleisen and M. Wolfsberg, *Advan. Chem. Phys.*, **1**, 15 (1958).

A first alternative to simply disregarding redundancy is to reduce it by elimination of excess internal coordinates. Structure E differs from D and G from F by subtraction of the angle bend coordinates 5 and 7; elimination of just the bond stretch coordinate 6 from F yields structure H. Because each of these coordinate eliminations affects \mathbf{G} subtractively but \mathbf{G}^{-1} in every term, we expect effects on $L(\text{TIF})$ and $L(\text{TDF})$ like those just recorded. Comparisons among columns 1–5 of Table V show this to be the case. Here the problem of $L(\text{TIF})$ interpretation is fundamentally different than with structure F, because the absence of redundancy in D, E, G, and H guarantees the correspondence in each case of the preselected reaction coordinate motion and the output reaction coordinate eigenvector; further, $\nu_1^\ddagger = 0$ in all cases. The different $L(\text{TIF})$ values obtained for identical \mathbf{L}_1 with structures D, E, G, and H emphasize the dependence of $L(\text{TIF})$ on \mathbf{G}^{-1} .

A second alternative to simply overlooking redundancy is to avoid its effects by transformation of the \mathbf{F} corresponding to a redundant \mathbf{G} to form corresponding to a nonredundant \mathbf{G} . For example, $(\mathbf{F}_R^\ddagger)_{\text{FKPU}}$ con-

Table VI. Original and Transformed Force Constant Matrices for the Case D/FXPU (Upper Right, $(F_R^0)_{FXPU}$; Lower Left, $(F_{NR}^0)_{D/FXPU}$)

j	i								j
	1	2	3	4	5	6	7	8	
	4.40	0	0	0	0	0	0	0	1
		4.40	0	0	0	0	0	0	2
1	5.73380		1.63	0	0	0	0	0	3
2	1.33381	5.73382		0.50	0	0	0	0	4
3	4.27959	4.27961	15.36133		0.25	0	0	0	5
4	1.33381	1.33381	4.27959	1.83381		0.50	0	0	6
5	2.82792	2.82794	9.07356	2.82792	6.24575		0.25	0	7
6	1.33380	1.33381	4.27959	1.33380	2.82792	1.33380		2.00	8
7	2.82793	2.82794	9.07357	2.82793	5.99575	2.82792	6.24575		

structured according to the coordinate definitions of G_F (redundant, R), would be transformed into, say, $(F_{NR}^\ddagger)_{D/FXPU}$ constructed according to the coordinate definitions of G_D (nonredundant, NR). F_{88} does not appear and is not even defined in the transformed force constant matrix, but the values of the elements of $(F_{NR}^\ddagger)_{D/FXPU}$ are such that the manifold of eigenvalues and eigenvectors of $G_D F_{NR}^\ddagger$ simulate the existence of coordinate 8 with $F_{88} = 2.0$ mdyn/Å; structure D behaves as if it were structure F.

The transformation is made subject to the condition that the potential energy be constant. Where S is the matrix of internal coordinates

$$(S_{NR})^T F_{NR} S_{NR} = 2V = (S_R)^T F_R S_R \quad (6)$$

Usually, $F = F^0$ and F^\ddagger is created after transformation by the methods described in section C above. F_R is usually diagonal but need not be. In any case, one may define a transformation matrix U between the sets of internal coordinates

$$S_R = U S_{NR} \quad (7)$$

such that

$$F_{NR} = U^T F_R U \quad (8)$$

To find U a sequence of steps is followed. Where ξ is the matrix of $3N$ cartesian displacement coordinates

$$S_R = B_R \xi \quad (9)$$

$$S_{NR} = B_{NR} \xi \quad (10)$$

and

$$B_R = U B_{NR} \quad (11)$$

There is a matrix²³ A_{NR} such that

$$B_{NR} A_{NR} = E \quad (12)$$

the identity matrix, or²⁴

$$A_{NR} S_{NR} = \xi \quad (13)$$

then

$$U = B_R A_{NR} \quad (14)$$

A more useful and illuminating relation for A_{NR} is²³

$$A_{NR} = M^{-1} (B_{NR})^T (G^{-1})_{NR} \quad (15)$$

where M^{-1} is the diagonal matrix of reciprocal particle

masses. The form of eq 8 actually employed in computation is

$$F_{NR} = [(G^{-1})_{NR} B_{NR} M^{-1} (B_R)^T] F_R [B_R M^{-1} \times (B_{NR})^T (G^{-1})_{NR}] \quad (16)$$

where i and j index coordinates common to G_R and G_{NR} , and k indexes coordinates appearing in G_R but not G_{NR} ; the elements of the original and transformed F matrices are related as follows (in the simple case where $F_{ik} = 0$)

$$(F_{ij})_{NR} = (F_{ij})_R + (F_{kk})(U_{ki} U_{kj}) \quad (17)$$

where

$$(U_{ki} U_{kj}) = \left[\sum_{m=1}^{3N} (B_{km})_R (A_{mi})_{NR} \right] \left[\sum_{m=1}^{3N} (B_{km})_R (A_{mj})_{NR} \right] \quad (18)$$

As an example, Table VI lists the elements of F_R^0 and F_{NR}^0 for the transformation D/FXPU. With $X = K$, columns 5 and 6 of Table IV list the transition state frequencies obtained with F_{NR}^\ddagger ; these are different in both value and isotope shift from the $(\nu_R^\ddagger)_j$ in columns 3 and 4, but it is important to note that the $(\nu_R^0)_i$ and the $(\nu_{NR}^0)_i$ are identical (and would be for any G_{NR} , i.e., for any complete set of coordinates based on the given masses and geometry). Columns 6 and 7 of Table V demonstrate the effects of two transformations on the factors of k/k' . $L(\text{TIF})$ is characteristic for each reaction coordinate of $(G^{-1})_{NR}$, here G_D^{-1} and G_H^{-1} . $L(\text{TDF})$, which columns 1–5 show to be insensitive to the differences among the $(G^{-1})_{NR}$ and, for this particular reaction coordinate, little dependent on the value of F_{88} , is drastically affected by the transformation. Given the size of some of the $(F_{ij})_{NR}$, Table VI, this is not surprising. Table VII indicates the expected dependence of such effects on the value of F_{88} .

II. Intermolecular Isotope Effects α

A. Temperature-Independent Factor in k/k' . The values of $L(\text{TIF})$ for intermolecular atom a isotope effects are collected in Table VIII (this type of isotope effect is designated α [see Table IB]; subscripts to α identify the reaction coordinate); their range is very great, 0.1–0.28L unit. $L(\text{TIF})$ is large only when atom a is part of a fragment of low mass (compare A, BK, CK, DK). Mass attachment away from atom a can increase $L(\text{TIF})$, but the increase depends markedly on the reaction coordinate (compare BK with BL, CK with CL, and the several DX with each other). Although the data are few, the results of given internal

(23) J. H. Schachtschneider, Technical Report No. 261–62, Project No. 31450, Shell Development Co., Emeryville, Calif., 1962.

(24) S. J. Cyvin, "Molecular Vibrations and Mean Square Amplitudes," Elsevier, Amsterdam, 1968.

Table VII. Intermolecular Isotope Effects α , Reaction Coordinate 1 (Influence of the Coupling Force Constant F_{88})

	Model				
	DKN	FKNZ ^a	D/FKNS	D/FKNT	D/FKNU
F_{88} , mdyn/A		10^{-4} -2.0	10^{-4}	1.0	2.0
$L(\text{TIF})$	0.8889	0.5756	0.8889	0.8889	0.8889
$L(\text{TDF}), \theta = 1$	0.3968	0.3968	0.3968	0.3350	0.2749
2	1.4305	1.4305	1.4304	1.1026	0.9767
3	2.8149	2.8149	2.8148	2.3094	1.8915
4	4.3556	4.3556	4.3554	3.5171	2.8881
5	5.9646	5.9646	5.9644	4.7504	3.9169

^a $\nu_1 \neq \leq 0.75 \text{ cm}^{-1}$; for all other cases $\nu_1 \neq = 0$.

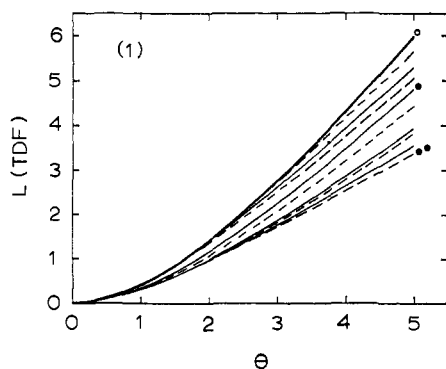


Figure 2. Temperature dependence of $L(\text{TDF})$, reaction coordinate 1, intermolecular isotope effects α : curve 1 (O), models A, BXN, CXY, DXN, and D/FKNS; curve 2, DXP, FKPU; curve 3, BXQ; curve 4, BXR; curve 5 (●), D/FKNT; curve 6, D/FJYU; curve 7, D/FKNU; curve 8, D/FKPU; curve 9, D/FMNU; curve 10 (●●), D/FMPU.

Table VIII. $L(\text{TIF})$ for Various Reaction Coordinates (Intermolecular Isotope Effects α ; Y = N, P, Q, R; Z = S, T, U)

Models	Reaction coordinate			
	1	2	12+	12-
A	2.5439	0.3682	1.8013	0.8568
BKY	0.7795	0.3957	0.6645	0.5816
BLY	0.1899	0.3444	0.1984	0.3139
CKY	2.6402	0.9732	2.0515	0.7935
CLY	2.7928	1.4105	2.3596	0.8461
DJY, D/FJYZ	1.7668	0.5543	1.3748	0.7690
DKY, D/FKYZ	0.8889	0.5786	0.8136	0.5338
DMY, D/FMYZ	0.1146	0.2388	0.1510	0.4381
EKY	1.0569	0.4550	0.9758	0.2123
FKNU	0.5756 ^a			
FKPU	0.5558 ^b	0.9641 ^b	0.8291 ^c	0.5338 ^d
GKPU	0.8545	0.5429	0.8320	0.2128
HKPU, H/FKPU	0.4469	0.1602		

^a $\nu_1 \neq = 0.75 \text{ cm}^{-1}$. ^b $\nu_1 \neq = 49.73 \text{ cm}^{-1}$. ^c $\nu_1 \neq = 58.29 \text{ cm}^{-1}$. ^d $\nu_1 \neq = 0.00021 \text{ cm}^{-1}$.

coordinate subtractions are similar (compare EK with DK and GK with FK) but depend on which subtraction is made (compare HK and GK with FK) and on the selection of reaction coordinate; attached mass coupling seems to have an opposite influence of similar magnitude (compare DK and FK). The small difference between the values for FKNU and FKPU (both of which are formally invalid because $\nu_1 \neq > 0$) is not primarily an eigenvalue effect but arises in the different patterns of contamination of the eigenvectors (see Table III).

B. Temperature Dependence of k/k' . Figures 2-5 show the graphs of $L(\text{TDF})$ vs. θ for each reaction coordinate. (The output data often show small differences; these are ignored in the figures and in the discussion

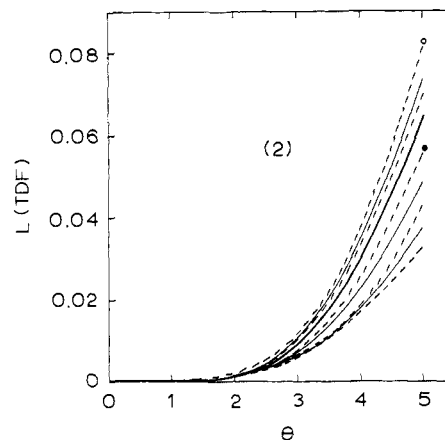


Figure 3. Temperature dependence of $L(\text{TDF})$, reaction coordinate 2, intermolecular isotope effects α : curve 1 (O), models D/FJYU; curve 2, BKQ; curve 3, BKR, DXP, FKPU; curve 4; A, BKN, BLY, CXY, DXN; curve 5 (●), D/FKPU; curve 6, D/FKNT; curve 7, D/FKNU; curve 8, D/FMPU; curve 9, D/FMNU.

where the related plots differ by less than twice the thickness of the curves themselves. The curves are numbered from the top down; to aid finding, the first curve terminates in an open circle, the fifth in a single spot, and the tenth in a double spot. Solid and broken curves alternate according to their position at $\theta = 5$ (except in Figure 6, *vide infra*) and the heavy solid curve always represents the results for structure A.

None of the mass attachments has a major influence on an isotope effect calculated with an untransformed F matrix; invariably, curves lying lower than the fourth or fifth are for the D/F transformations of some $F_{88} \neq$. But, at ordinary laboratory temperatures (θ ca. 3) the span of $L(\text{TDF})$ values from curves 1 through 4 or 5 is several times the experimental imprecision of ordinary ^{13}C isotope effect measurements.

The observations arise, of course, in the primary dependence of $L(\text{TDF})$ on force constant changes between the reactant and transition states and in the invariance of the elements of ΔG from one structure to another. $L(\text{TIF})$ does not show this behavior because any change in structure affects many elements of G^{-1} . For $L(\text{TDF})$, this is what one would expect from the work which led Stern and Wolfsberg²¹ to develop the "cut-off" procedure (based on observation that structural elements more than one or two atoms distant from the position of isotopy have but small effect on calculated kinetic isotope effects, provided they are excluded from the reaction coordinate);¹⁶ our approach in this investigation is the reverse, *i.e.*, to "add on."

$\Delta G_{22} = 0$ for isotopy at atom a (Table II) and the very

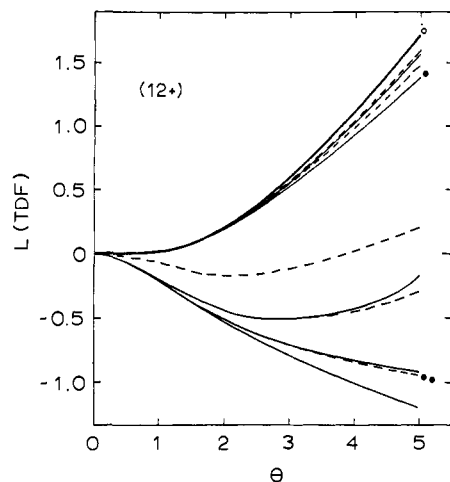


Figure 4. Temperature dependence of $L(\text{TDF})$, reaction coordinate 12+, intermolecular isotope effects α : curve 1 (O), models A, BKN, BLY, CXY, DXN, DMY, D/FKNS; curve 2, DJP; curve 3, DKP, FKPU; curve 4, BKQ; curve 5 (●), BKR; curve 6, D/FKNT; curve 7, D/FJNU; curve 8, D/FJPU; curve 9, D/FKNU; curve 10 (●●), D/FKPU; curve 11, D/FMNU, D/FMPU.

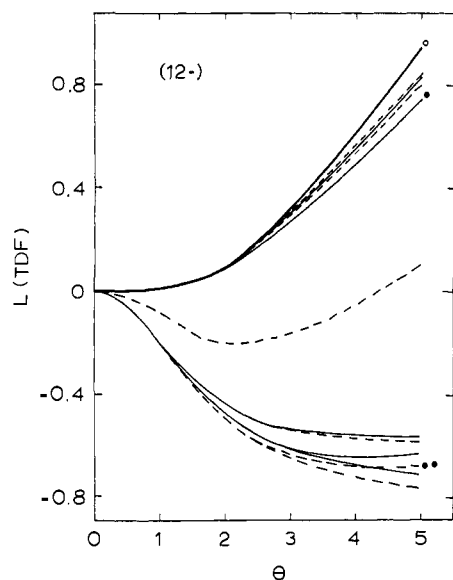


Figure 5. Temperature dependence of $L(\text{TDF})$, reaction coordinate 12-, intermolecular isotope effects α : curve 1 (O), models A, BKN, BLY, CXY, DXN, DMY, D/FKNS; curve 2, DJP; curve 3, DKP, FKPU; curve 4, BKO; curve 5 (●), BKR; curve 6, D/FKNT; curve 7, D/FJNU; curve 8, D/FJPU; curve 9, D/FKNU; curve 10 (●●), D/FMNU; curve 11, D/FKPU; curve 12, D/FMPU.

small values for $L(\text{TDF})$ represented by the plots of Figure 3 reflect that fact. We defer to a later section consideration of the effects of $F_{\mathbf{R}}^{\pm}$ transformations, but it is apparent from Table V that redundancy and coordinate subtraction create problems of interpretation with respect to $L(\text{TIF})$, while the reduction of redundancies *via* transformation creates similar problems with respect to $L(\text{TDF})$. $L(\text{TDF})$ is largest for simple a-b bond rupture (reaction coordinate 1) and either concerted motion (compare Figures 4 and 5 with Figure 2) yields a lower value. However, this is *not* a general effect of increasing the complexity of the reaction coordinate motion because of the widening range of eigenvector element ratios related thereto.^{10,18,19}

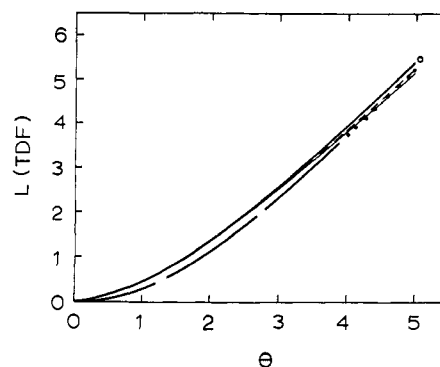


Figure 6. Temperature dependence of $L(\text{TDF})$, $\theta = 1000/T^{\circ}\text{K}$, various reaction coordinates, intermolecular isotope effects β : models A, BJN, BJP, BKN, BKP, BMN, BMP, DJN, DJP, DKN, DKP, DMN, DMP; curve 1 (—O), reaction coordinate 1, all models; reaction coordinate 2, all models except BXP (*i.e.*, BJP, BKP, BMP); curve 2 (—, extended by ···), reaction coordinate 12-, all models; curve 3 (- -), reaction coordinate 2, models BJP and BKP; curve 4 (—), reaction coordinate 2, model BMP. (See notes to Table X for comparison of results for structures B and C.)

Table IX. Summary for Intermolecular Isotope Effects α of the Influence on $L(\text{TIF})$ and $L(\text{TDF})$ of Increases in Attached Masses and Attachment and Coupling Force Constants

Reaction coordinate	Models	$-\Delta L(\text{TIF})^c$		$-\Delta L(\text{TDF})^c$	
		m_x^+	m_z^+	f_y^+	f_z^+
1	BXY	- ^a	0	- ^b	
	CXY	(+)	0	0	
	DXY, D/FXYZ	-	-	-	-
2	BXY	(-)	(+)	(+) ^d	
	CXY	+	0	0	
	DXY, D/FXYZ	-	(-)	(+)	(-)
12+	BXY	-	(-)	(-) ^d	
	CXY	+	0	0	
	DXY, D/FXYZ	-	-	-	-
12-	BXY	-	(-)	- ^d	
	CXY	(+)	0	0	
	DXY, D/FXYZ	-	- ^e	-	-

^a Read: $L(\text{TIF})$ decreases when the mass represented by a symbol at X increases. ^b Read: $L(\text{TDF})$ decreases when the force constant represented by a symbol at Y increases. ^c Effects much smaller than the average for a given reaction coordinate are indicated by parentheses. ^d The effect of f_y decreases with increasing m . ^e After initial (+).

C. Observations on k/k' . Table IX is a summary of the attached mass and force constant effects detailed in Table VIII and Figures 2-5, designed to assist consideration of the influence of such variations on k/k' . Experimentally, one cannot separate $L(\text{TIF})$ from $L(k/k')$, though measurements at very high temperatures can yield an approximate value since $L(\text{TDF})$ should be small. By the same token, $L(\text{TDF})$ cannot be determined, but its temperature dependence is always accessible and can often be measured accurately. Interpretations of a kinetic isotope effect start with the average magnitude of the quantity and, one hopes, its dependence on temperature over some modest range of experimental conditions.

Large $L(\text{TDF})$'s do not usually exhibit small temperature dependence over ranges of 50-100° near 350°K.^{13,25,26} Under such conditions a large $L(k/k')$ rather insensitive

(25) M. J. Stern, W. Spindel, and E. U. Monse, *J. Chem. Phys.*, **48**, 2908 (1968).

(26) W. Spindel, M. J. Stern, and E. U. Monse, *J. Chem. Phys.*, **52**, 2022 (1970).

to temperature would seem to indicate a large $L(\text{TIF})$. Such observations could result except for reaction coordinate 1 from any of the models employed in this study. According to Tables VIII and IX, the most favorable cases involving some complexing (mass attachment) are structure C with high masses and structure D with low masses for reaction coordinates 1 and 12+; chemically, reaction coordinates like 12+ are not very likely to occur. If changes of reaction medium are observed to alter $L(k/k')$, these results suggest that the effect is on $L(\text{TIF})$ rather than $L(\text{TDF})$, and the shift observed could be interpreted in terms of changes in complexing *via* results like those in Table VIII.

IV. Intermolecular Isotope Effects β

A. $L(\text{TIF})$. More often than not the attached mass effects on $L(\text{TIF})$ for β (see Table IB) intermolecular isotope effects (see Table X) are opposite those

Table X. $L(\text{TIF})$ for Various Reaction Coordinates (Intermolecular Isotope Effects β ; Y = N, P)

Models	Reaction coordinate			
	1	2	12+	12-
A	1.0558	1.0558	0.3865	2.2457
BJY	0.9768 ^a	0.9485 ^b	0.4049 ^c	1.9301 ^c
BKY	1.1848	0.8490	0.5235	2.0162
BMY	1.8409	0.7112	1.0052	2.5333
DJY	0.9136	0.9136	0.3540	1.9412
DKY	0.8421	0.8421	0.2732	2.2407
DMY	0.3320	0.3320	0.7016	2.9186

^a Same as CJY, reaction coordinate 2; etc. ^b Same as CJY, reaction coordinate 1; etc. ^c Same as CJY; etc.

found for the comparable α intermolecular cases (compare Tables IX and X); the span of the β -type values is greater in the case of structure B and smaller for structure D. There are in these limited examples no obvious effects of the higher symmetry of the β situation than the α , beyond the identity of the $L(\text{TIF})$'s for reaction coordinates 1 and 2 when structure D is employed.

B. $L(\text{TDF})$. Figure 6 collects the $L(\text{TDF})$ vs. θ curves for structures A, B, and D, and reaction coordinates 1, 2, and 12-. All of these isotope effects are large, strongly dependent on temperature (all are of Stern, Spindel, and Monse's type A²⁵), and without substantial dependence on the occurrence of complexing. These properties arise primarily in the greater removal of atom b than that of atom a from the sites of attachment and secondarily in the higher symmetry of the β mass pattern than the α . The values of $L(\text{TDF})$ for the symmetric reaction coordinate 12+ are very small; see Figure 7. Those for structures A and D would be zero if the first-order high-temperature approximation²² were valid here. The origin of these second-order effects on type II results has been detailed elsewhere.^{16,17}

C. **Observations on k/k' .** Table XI summarizes the attached mass and complexing force constant effects detailed in Table X and Figures 6 and 7. For these β intermolecular isotope effects, only the essential absence of temperature dependence of $L(k/k')$ associated with reaction coordinate 12+ and the very large values predicted for less symmetric reaction coordinates (e.g., $L(k/k')$ corresponds to an approximately 5% ¹³C iso-

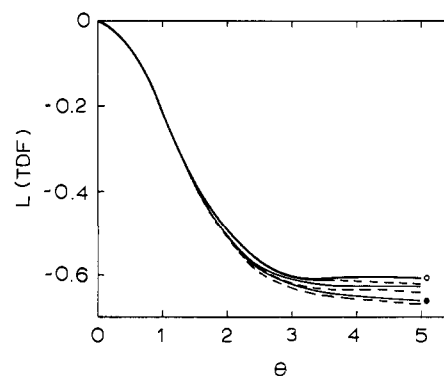


Figure 7. Temperature dependence of $L(\text{TDF})$, reaction coordinate 12+, intermolecular isotope effects β : curve 1 (O), model A; curve 2, models BJN, BMN, DXN (i.e., DJN, DKN, DMN); curve 3, BJP, BMP; curve 4, DXP; curve 5 (●), BKN; curve 6, BKP. (See notes to Table X for comparisons of results for structures B and C.)

Table XI. Summary for Intermolecular Isotope Effects β of the Influence on $L(\text{TIF})$ and $L(\text{TDF})$ of Increases in Attached Masses and Attachment Force Constants

Reaction coordinate	Models	ΔL		
		m_x^+	m_x^+	f_y^+
1	BXY ^a	+	0	0
	DXY	-	0	0
2	BXY ^b	-	(-) ^c	0
	DXY	-	0	0
12+	BXY,CXY	+	0	0
	DXY	+ ^d	0	0
12-	BXY,CXY	+	0	0
	DXY	+	0	0

^a Same as CXY, reaction coordinate 2. ^b Same as CXY, reaction coordinate 1. ^c The mass effect increases with increasing f_y . ^d After initial (-).

tope effect at 100°) are significant features. The lower span of β -type $L(\text{TIF})$ values coupled with the likelihood of large $L(\text{TDF})$'s makes such isotope effects less attractive than the α type for exploration of solvent and complexing effects.

IV. Intramolecular Isotope Effects γ

The results for intermolecular isotope effects of types α and β discussed in sections II and III can be combined in various ways to yield data on the *intramolecular* isotope effects (γ) which arise in isotopy at bifunctional groups or in other ways determined by molecular symmetry. The investigation of such isotope effects is convenient because they persist at complete reaction and can, therefore, be determined from isotope fractionation measurements over any integral or differential degree of reaction. Conversely, determination of *intermolecular* isotope effects becomes increasingly difficult past low degrees of reaction.

A. $L(\text{TIF})$. Data on the temperature-independent factor for four types of effects are collected in Table XII. Because many combinations of intermolecular effects yield intramolecular isotope "effects" which are null by definition, the useful comparisons are few.

$L(\text{TIF})$ can be of either sign. (The mass pattern for γ effects was defined so that $L(\text{TDF}) \geq 0$ in most cases.) As a result, intramolecular isotope effects can exhibit inversion in the sign of $L(k/k')$ without $L(\text{TDF})$ exhibiting any of the anomalies of temperature dependence described by Stern and his colleagues.^{11,25,26}

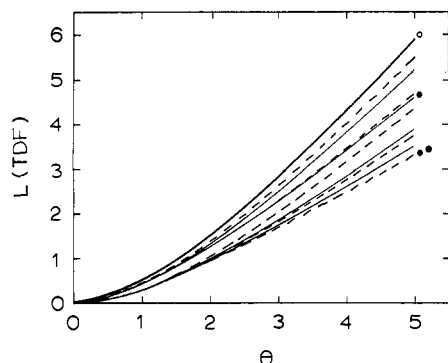


Figure 8. Temperature dependence of $L(\text{TDF})$, intramolecular isotope effects $\gamma = \alpha_1/\alpha_2$, $\alpha_1(\text{BXQ})/\alpha_2(\text{CXQ})$, and $\alpha_1(\text{CXQ})/\alpha_2(\text{BXQ})$: curve 1 (O), models A, (CKQ/BKQ), (CLQ/BLQ), DJN, DKN, DMN, D/FKNS; curve 2, DJP, DKP, DMP, EKP, FKPU, GKPU, HKPU; curve 3, (BKQ/CKQ), (BLQ/CLQ); curve 4, D/FKNT; curve 5 (●), H/FKPU; curve 6, D/FJNU, D/FJPU; curve 7, D/FKNU; curve 8, D/FKPU; curve 9, D/FMNU; curve 10 (●●), D/FMPU. $L(\text{TDF}) \leq 0$ for all intramolecular isotope effects calculated of types $\gamma = \alpha_{12+}/\alpha_{12+}$, $\alpha_{12-}/\alpha_{12-}$, β_1/β_2 ; because $L(\text{TDF}) \cong -0.04$ at $\theta = 3$ and ~ -0.2 at $\theta = 5$, the results are not plotted.

Table XII. $L(\text{TIF})$ for Various Intramolecular Isotope Effects γ

"Inter" type and reaction coordinate	Models	$L(\text{TIF})$
$\gamma = \alpha_1/\alpha_2^a$	A	2.1757
	(BKY/CKY) ^b	-0.1937
	(BLY/CLY)	-1.2206
	(CKY/BKY)	2.2445
	(CLY/BLY)	2.4484
	DJY, ^c D/FJYZ	1.2125
	DKY, D/FKYZ	0.3103
	DMY, D/FMYZ	-0.1242
	EKY	0.6019
	FKPU	-0.4083
	GKPU	0.3116
	HKPU, H/FKPU	0.2867
	$\gamma = \alpha_{12+}/\alpha_{12+}$	(BKY/CKY)
(BLY/CLY)		-2.1612
$\gamma = \alpha_{12-}/\alpha_{12-}$	(BKY/CKY)	-0.2119
	(BLY/CLY)	-0.5323
$\gamma = \beta_1/\beta_2$	A	0.0
	BJN, BJP	0.0283
	BKN, BKP	0.3359
	BMN, BMP	1.1297

^a Read: $(k/k')_\gamma = (k/k')_{\alpha_1}/(k/k')_{\alpha_2}$. ^b Read: $\gamma = \alpha_1(\text{BKY})/\alpha_2(\text{CKY})$. ^c Read: $\gamma = \alpha_1(\text{DJY})/\alpha_2(\text{DJY})$.

Where there is but one attached mass (as in structures B and C), $|L(\text{TIF})|$ increases as that mass increases for all four types. (As may be seen from the results for $L(\text{TDF})$ presented below, some of the negative $L(\text{TIF})$'s are so large that the resulting $L(k/k')$ would be small at temperatures near 60° (θ ca. 3.0) and yet exhibit very great temperature dependence.) Effects of coordinate subtraction are not consistent in sense (compare EK with DK and GK with FK and section II.A).

B. $L(\text{TDF})$ and $L(k/k')$. Of the four types of intramolecular isotope effects calculated, only α_1/α_2 exhibits $L(\text{TDF})$ of substantial magnitude; these results are collected in Figure 8. None of the $|L(\text{TDF})|$ for $\alpha_{12+}/\alpha_{12+}$, $\alpha_{12-}/\alpha_{12-}$, and β_1/β_2 exceeds 0.3 at $\theta = 5$; because $L(\text{TIF})$ in these cases can be large, there is the possibility in situations of unsymmetrical complexing that $L(k/k')$ be large and virtually independent

of temperature over a wide range of temperature. Together with the consequences of $L(\text{TIF}) < 0$, this observation suggests that the intramolecular isotope effect is an especially useful tool for study of complexing and medium interaction effects; compare Table XIII with Tables IX and XI. Part of this utility lies in

Table XIII. Summary for Intramolecular Isotope Effects γ of the Influence on $L(\text{TIF})$ and $L(\text{TDF})$ of Increases in Attached Masses and Attachment and Coupling Force Constants

"Inter" type and reaction coordinate	Models	$\Delta L(\text{TDF})$			
		m_x^+	m_x^+	f_y^+	f_z^+
$\gamma = \alpha_1/\alpha_2$	(BXY/CXY)	-	0		
	(CXY/BXY)	+	0		
	DXY, D/FXYZ	-	-	-	-
$\gamma = \alpha_{12+}/\alpha_{12+}$	(BXY/CXY)	-	(+)		
	(BXY/CXY)	(-)	(+)		
$\gamma = \beta_1/\beta_2$	BXY	+	+	(+)	

the independence of the intramolecular isotope effects on properties of the reactant state; this permits certain consequences of activation to be revealed by comparison of the related *inter*- and *intramolecular* effects.

V. Comparisons and Conclusions

A. α and β Intermolecular Isotope Effects, SMM.

The range of $L(\text{TIF})$, given a comparable group of models, is smaller for the β effects than for the α (compare Tables VIII and X), but except for the molecular fragment basis²² for values in the cases of reaction coordinates (1) and (2), eq 5 permits no easy understanding of $L(\text{TIF})$ even for two-element reaction coordinates.

$L(\text{TDF})$ for the β isotope effects reflects the symmetric location of atom b in the TAM "molecule;" both internal coordinates 1 and 2 are isotopic for the β but only 1 for the α intermolecular effects. For reaction coordinates (1), (2), and (12-) in β , and (1) in α , the $L(\text{TDF})$'s are strikingly similar (Figures 2 and 6). This quantity for (12+) in the β mass pattern (Figure 7) is very small and obviously does not have its origin primarily in "bond ruptures." The small size of the α isotope effect for reaction coordinate 2 (Figure 3) is traceable to the nonisotopic character of that internal coordinate, and its function as a "diluent" element of (12+) and (12-) (Figures 4 and 5) cannot be doubted.

Except for the trivial α isotope effect for reaction coordinate 2, mass attachment always lowers $L(\text{TDF})$, but the effects are small. This means that only crude information concerning complexing or similarly strong medium-reactant interaction could be obtained from the determination of temperature dependence of an isotope effect under one set of experimental conditions. However, the effects of SMM parameter variations are sufficiently great that useful information about such interactions should result from comparison of temperature dependences obtained under several different sets of conditions (for example, from measurements on the same reaction in different solvents, on salt effects, etc.).

B. Intramolecular Isotope Effects, SMM. The intramolecular isotope effects obtained with an untransformed F (whether shown or not in Figure 8) belong to just two major groups: those with $|L(\text{TDF})|$ large and small. The large effects are of the type $\gamma = \alpha_1/\alpha_2$ and

the small of the types $\gamma = \alpha_{12+}/\alpha_{12+}$, $\alpha_{12-}/\alpha_{12-}$, β_1/β_2 . All of the examples discussed here are derived directly from independently calculated α and β intermolecular effects. Earlier it was seen that α_1 effects (*i.e.*, intermolecular isotope effects for mass pattern α with reaction coordinate 1) are generally large and α_2 effects almost negligible (Figures 2 and 3); $\gamma = \alpha_1/\alpha_2$ will be much like α_1 . The β_1 and β_2 effects (Figure 6) never differ by much, so $\gamma = \beta_1/\beta_2$ is always nearly zero. The α_{12+} and α_{12-} intermolecular effects are affected somewhat by mass attachment and coupling, but the shifts are not large and combination of any pair into an intramolecular isotope effect results in $L(\text{TDF})$ always small.

These features of temperature dependence and the possibility that $L(\text{TIF}) < 0$ suggest that paired determinations of intermolecular and intramolecular isotope effects could be peculiarly useful in establishing the nature and magnitude of solvent-solute interactions on kinetic isotope effects. This is not exactly a novel idea,^{27,28} but SMM appears to offer a convenient formalism for the expression and interpretation of such differential magnitudes. Such determinations could provide sensitive tests of the comparative validity of SMM and CMM at various levels of reactant-medium interaction.

C. Redundancy and Reaction Coordinate Simplicity, SMM. None of the discussion presented thus far in this section applies to $L(\text{TDF})$ for transformation cases D/F or any like them. It is obvious from Figures 2-5 and 8 that F^\ddagger transformations to simulate the effect of F_{88} without defining it in G_{NR} have effects on $L(\text{TDF})$ enormously greater than any arising as a direct consequence of mass attachment or coupling. As detailed in section II.D, the transformation technique was employed because of the serious eigenvector contamination resulting from coordinate redundancy (Table III). But, it is apparent from the data of Tables V and VII that F_{R}^\ddagger transformation is a drastic overreaction to the eigenvector problem unless the coupling force constant F_{88} is so low as to be without major consequence. (The problem is that of the augmentation of a canonical bond structure. For example, an intramolecular hydrogen bond included in G makes a kinematically complete set of internal coordinates redundant; the situation could be corrected either by underdefinition of the basis G , by subtraction of an uninteresting coordinate, or by a transformation of G_{R} so that the hydrogen bond would be simulated. Here, the transformation D/F when $F_{88} = 2.0$ is like simulating in a bent propene one of the C-C bonds of cyclopropane. Transformation of a weaker bond would have a more reasonable result; compare the data for FKPU, D/FKPU, and H/FKPU in Table V.)

Thus, an interesting operational question is exposed; where eigenvector preselection is believed important to the development of understanding of the relation between reaction coordinate motions and kinetic isotope effects, what price in unrealistic F matrix elements or in underdefinition of coordinate structure is reasonably paid to avoid eigenvector contamination?

Guided by the philosophy of the "cut-off" pro-

(27) P. E. Yankwich and R. L. Belford, *J. Amer. Chem. Soc.*, **76**, 3067 (1954).

(28) P. E. Yankwich and H. S. Weber, *J. Amer. Chem. Soc.*, **78**, 564 (1956).

cedure,²¹ the proper answer to this question seems obvious to us: Where one is computing isotope effects but not rates, underdefinition of an internal coordinate set by subtraction of angle bend coordinates is preferable to transformation of F_{R}^\ddagger to F_{NR}^\ddagger so that G_{NR} can be employed. One cannot, of course, subtract a coordinate one wishes to use as an element of a complex reaction coordinate, and the subtraction must be done consistently for reactant and transition states.

D. Molecular Mass and Complexity, CMM and SMM. As noted in the introduction, CMM medium-induced ^{13}C isotope fractionation decreases with molecular mass and complexity; carbon is a skeletal atom and increasing molecular bulk removes positions of possible isotopy progressively from the molecular exterior. Results reported in the first paper in this series² showed average CMM effects on formic acid to be about 0.70 and on oxalic acid to be about 0.15 those on TAM.

The SMM results reported here present several opportunities for estimate of such effects. The behavior of $L(\text{TIF})$ with respect to the structure variations in models A, BXY, and DXY (Tables VIII and X) is too complex to be determined from the number of comparisons available, so discussion will be limited to $L(\text{TDF})$.

Atoms a and b are dissimilarly situated in the model molecule, yet most β intermolecular $L(\text{TDF})$'s are similar to the largest of the α family. Comparison of the α_{12+} results with the β_{12+} graphs for $L(\text{TDF})$ (Figures 4 and 7) shows, as does comparison of related α_{12-} and β_{12-} (Figures 5 and 6), that in a small model molecule like TAM the relative position of isotopic coordinates has more influence on the magnitudes of isotope effects than their simple identity.

For isotope effects of a given type, the influences of mass attachment and coupling do depend on the location of the isotopic position; the complexing induced shifts of α intermolecular isotope effects are consistently larger than those found with the β (compare Figures 2 and 6) of similar magnitude. Indeed, β isotope effects are insensitive to molecular business beyond atoms a and c, a result entirely consistent with Stern and Wolfsberg's "cut-off" modeling.^{20,21}

E. CMM and SMM. The TAM calculations published earlier² were for CMM intermolecular α isotope effects; numerous comparisons are possible to some of the SMM results reported here. Table XIV shows $L(\text{TIF})$ values and those of $L(\text{TDF})$ at $\theta = 3$ for a number of external models. The modification of G required by definition of three translational and three rotational external coordinates in CMM produces a small shift in $L(\text{TIF})$ from "gas phase" values of no practical significance given present experimental techniques for ^{13}C . (Many small shifts like these would be magnified enormously if our model were for H/D isotopy and perhaps be conveniently measurable.) $L(\text{TIF})$ values are very different for the SMM models shown here and for others discussed earlier. Because $L(\text{TIF})$ depends on G^{-1} , different SMM model structures may yield very different $L(\text{TIF})$'s for the same reaction coordinate motion.

All of the temperature-dependence graphs $L(\text{TDF})$ vs. θ for the models listed in Table XIV are simple monotonic functions (type A of Stern, *et al.*²⁵). For

Table XIV. Comparison of TAM Calculated Intermolecular Isotope Effects α for "Gas Phase" and Several CMM and SMM Models

	Reaction coordinate			
	(1)	(2)	(12+)	(12-)
(A) $L(\text{TIF})$				
(1) Gas phase	2.5439	0.3682	1.8013	0.8568
(2) CMM	2.6143	0.3798	1.8503	0.8849
(3) (a) SMM (DKP)	0.8889	0.5786	0.8136	0.5338
(b) SMM (FKPU)	0.5558	0.9641	0.8291	0.5338
(B) $L(\text{TDF})$ at $\theta = 3$ (60.17°)				
(1) Gas phase	2.8149	0.0093	0.5991	0.3294
(2) (a) CMM ($\varphi_3 \neq \varphi_3^0$) ^a	2.8150	0.0093	0.5991	0.3295
(b) CMM ($\varphi_3 \neq \varphi_3^0$) ^b	2.7876	-0.0182	0.6207	0.3020
(c) CMM ^a (max $e - e$) ^c	2.8151	0.0093	0.5991	0.3295
(d) CMM ^a (max $e - i$, F_{3,T_z}) ^d	2.8705	0.0648	0.6546	0.3800
(e) CMM ^b (F_{3,T_z}) ^e	2.8431	0.0373	0.6762	0.3575
(3) (a) SMM (DKP)	2.7267	0.0100	0.5696	0.3086
(b) SMM (FKPU)	2.7287	0.0136	0.5738	0.3087

^a In φ_3 , the several $F_{\text{translations}} \approx 0.16$ mdyne/Å and the $F_{\text{rotations}} \approx 0.02$ (mdyne Å)/rad², in the external force field. ^b The φ_2 force constants are one-half the φ_3 . ^c The external-external interaction force constant $F_{T_z, T_y} = 0.159$, just below the value (0.160) which yields an additional nongenuine vibration. ^d The external-internal interaction force constant $F_{3, T_z} = 0.510$, just below the value (0.511) which yields an additional nongenuine vibration. ^e As in (2b), but with F_{3, T_z} near maximum value.^d

convenience, we compare results at the single temperature $\theta = 3$; some of the differences increase substantially as θ increases. In CMM, medium effects are nil if the states of medium striction about the reactant and transition states are the same, in the absence of coordinate interaction effects (compare B.1 and B.2a in Table XIV). Introduction of differences of striction (compare B.2a and B.2d in Table XIV) and of external-internal coordinate interactions (the internal coordinate is not included in the reaction coordinate) (compare B.2a and B.2d, B.2b and B.2e in Table XIV) yield effects below the limit of detection except where, as possibly with reaction coordinate 2, the perturbation causes a change in the character of the temperature dependence; even so, one would want independent chemical or physical evidence before attributing such a result to this source. The consequences of interaction among the external coordinates (compare B.2a and B.2c in Table XIV) are negligible. In SMM and with light attached masses, attachment constants of size comparable to typical CMM "external" force constants yield medium effects on $L(\text{TDF})$ an order of magnitude larger. Most of this difference is due to the fact that the corresponding elements of the two ΔG differ in the same manner. Medium effects according to SMM are intrinsically larger than those according to CMM for this reason.

F. SMM Medium Effects. The computational experiments reported here employ the masses of attached particles and the force constants related to their attachment and coupling as parameters. Coupling does not appear to have major influence on $L(\text{TDF})$ for models involving coordinates removed from the coupling site (compare 3a and 3b, Table XIV), but both the attached

mass and the force constant related to the attachment have significant influence under certain conditions. This suggests that a medium of low rigidity might (for purposes such as those of this work) be represented simply as a small set of attachable mass points, but, something as rigid as an enzyme, for example, would surely require that the coupling parameter be investigated more thoroughly.

Although potentially large in comparison with those obtained *via* CMM, SMM *medium* isotope effects are not predicted to be so large that their presence or absence could be inferred directly; comparison experiments would still be required. Within the framework of SMM there are useful effects on both $L(\text{TIF})$ and $L(\text{TDF})$ in the case of intramolecular isotope effects; the utility of the $L(\text{TDF})$ shifts would be less for intermolecular effects when, as here, neither the attachment nor the coupling internal coordinates are incorporated in the reaction coordinate. In CMM, $L(\text{TIF})$ is an insensitive quantity.

The implications for experimental work of these two approaches to modeling the physical interaction of medium with reactant are that: if the assumptions of CMM are valid, experimentally determined heavy-atom kinetic isotope effects are essentially free of a medium-induced component, and computational techniques appropriate to gas phase systems may be employed to model the dynamic process; whereas, if the assumptions of SMM are valid, such experimental results may have an appreciable medium-induced component, and an additional problem for reaction modeling is the estimation and separation of the physical and chemical contributions to the isotope effects observed.

However, reactant-medium interactions so strong as to affect the reaction coordinate, diagonal force field, or both should have effects on $L(\text{TDF})$ in both SMM and CMM much larger than those discussed in this report. Again, SMM is expected to yield the larger shifts from the no-interaction values because of larger elements in the extrareactant parts of ΔG . A series of isotope effect measurements on one reaction in a number of different solvents should permit one to discover the conditions under which CMM and SMM yield equally reasonable representations of the chemical situations and those under which one or the other approach is to be preferred. The task could be speeded were a bifunctional reagent used, since both the intermolecular and intramolecular isotope effects would be obtainable. Interactions which are "strong," as defined just above, yield similar situations experimentally in either the CMM or SMM framework; interaction and dynamic effects are inextricably combined. But, the intrinsic magnitude of the former is so small in comparison to the latter that it can often be neglected, making the interpretation of experiments a *kinetic* isotope effects problem, though one of somewhat greater complexity than for reaction in the gas phase.

Acknowledgment is made to the donors of the Petroleum Research Fund, administered by the American Chemical Society, for the support of this research.